Geophysical Research Letters®

Key Points:
- The tropopause dust layer covers a full circuit around the globea
- The Ethiopian Plateau and the Rocky Mountains are two new transport pathways of the GTDL
- The contribution of dusts from IND to GTDL is the largest and the one from NAF to GTDL is the smallest

A Simulation Study on the New Transport Pathways of Global Tropopause Dust Layer

Qingzhe Zhu[1], Yuzhi Liu[1,2], Tianbin Shao[1], Run Luo[1], and Ziyuan Tan[1]

[1]Key Laboratory for Semi-Arid Climate Change of the Ministry of Education, College of Atmospheric Sciences, Lanzhou University, Lanzhou, China, [2]Collaborative Innovation Center for Western Ecological Safety, Lanzhou University, Lanzhou, China

Abstract Previous study of the tropopause aerosol layer is focused on the region surrounding the Tibetan Plateau. However, other transport pathways of the tropopause aerosol layer remain unclear. In this study, by simulating the dusts from different dust sources individually, we detected the Ethiopian Plateau and the Rocky Mountains are two new transport pathways of the global tropopause dust layer (GTDL). In addition, the contributions of different dust sources to the GTDL were quantified, the mass concentration percentage of dusts originating from Indian Peninsula in the GTDL at 100 hPa is 31.5%, which is the largest, followed by those of dusts from Middle East and Northwestern East Asia, dusts from North Africa contribute 17.3% to the GTDL at 100 hPa, which is the smallest. Our results demonstrate the existence of multiple transport pathways of the tropopause aerosol layer and clearly provide the contributions of each dust source to the GTDL.

Plain Language Summary Tropospheric aerosols can be transported through specific regions to the stratosphere. The current studies indicate the TP as a key region for aerosol transport. Through model simulations, in this study, we found that the Ethiopian Plateau in Africa and the Rocky Mountains in North America are also the pathways for aerosol transport. We also found the contribution of dusts originating from Indian Peninsula to the GTDL is the largest, followed by dusts originating from Middle East and Northwestern East Asia, and the contribution of dusts originating from North Africa to the GTDL is the smallest.

1. Introduction

The tropopause, as the unique region between the troposphere and the stratosphere, located between 200 and 50 hPa (12–16 km above sea level) (Hoinka, 1997; Holton et al., 1995), plays an important role in the transport of materials from the troposphere to the stratosphere (Dessler et al., 2013; Fu et al., 2006; Randel & Jensen, 2013). Satellite observations have indicated trace gas originating from troposphere can be detected in the tropopause (Kar et al., 2004; Park et al., 2004; Randel et al., 2010). However, the observations of the troposphere aerosols by satellites were very sparse in the early days, and only the simulations showed that aerosols can be transported to the troposphere through the Tibetan Plateau (TP) (Li et al., 2005). With the Cloud-Aerosol Lidar and Infrared Pathfinder Satellite Observation (CALIPSO) satellite was launched in 2006 (Winker et al., 2009), the study of the tropopause aerosol layer (TAL) was confirmed and developed. The existence of a TAL spanning the Middle East to East Asia between 13 and 18 km called the Asian tropopause aerosol layer (ATAL) in summer was discovered by the CALIPSO observations (Vernier et al., 2011, 2015), which has greatly promoted the studies in this subject.

The dynamics of the TAL formation is a widely concerned issue. Previous studies noted concentration of ATAL during the Asian Summer Monsoon (ASM) period is significantly stronger than that during the premonsoon period (Frey et al., 2015; Lau et al., 2018; Yuan et al., 2019), and many studies have identified strong updrafts and deep convections during the ASM period are important factors in the formation of the ATAL (Fadnavis et al., 2013; Neely et al., 2014; Pan et al., 2016; Vogel et al., 2015; Yu et al., 2015). In addition, the transport pathway of TAL is also widely discussed. In many studies, the TP is considered as a transport pathway due to its strong updrafts (Bian et al., 2020; Fadnavis et al., 2013; Lau et al., 2018; Legras & Bucci, 2020; Tissier & Legras, 2016), Lau et al. (2018) highlighted the Himalayas-Gangetic Plain over the southern TP and the Sichuan Basin over the eastern TP are transport pathways due to the deep convections. As

for the origin of the TAL, some studies suggested that India, the TP, southwestern China, and Southeast Asia are the sources of the ATAL (Bergman et al., 2012; Fadnavis et al., 2014; Fairlie et al., 2020; Park et al., 2009; Vogel et al., 2015; Wen et al., 2021). However, due to most studies on aerosols transport to the tropopause focused on the regions around the TP, other possible transport pathways of the TAL are unclear. In addition, the contribution of different aerosol sources to the TAL has not been quantified.

Previous studies have found that dust aerosol is a component of the TAL, and some of them showed that dust aerosol is the dominant aerosol by mass in the TAL (Bossolasco et al., 2021; Fadnavis et al., 2013; Gu et al., 2016; Lau et al., 2018; Ma et al., 2019; Xu et al., 2015; Yuan et al., 2019). Satellite observations have revealed dusts can circle around the Northern Hemisphere in the upper troposphere (Chao et al., 2018). Combining satellite observations and simulations, it has been observed that dusts originating from Tak-limakan Desert can be lofted to around 8–10 km above the surface and transported through a full circuit around the globe (Uno et al., 2009). These results suggest that the tropopause dust layer is over a global scale, therefore, in this study, we focus on the transport pathways and formations of the global tropopause dust layer (GTDL).

This study aims to quantify the contributions of the main dust sources to the GTDL and to search for new transport pathways. Using the coupled Nonhydrostatic ICosahedral Atmospheric Model (NICAM), we separated the dusts originating from different sources and obtained the spatial distributions and profiles of dust mass concentration for each dust source. Based on the 3D distributions of dust mass concentration, we identified new transport pathways besides the TP. In addition, the dust mass concentration proportions of different dust sources in vertical layers are calculated, which allows to better understand the variation of dust originating from each dust source in the vertical direction and to quantify their contributions to the GTDL.

2. Materials and Methods

2.1. Satellite Observations and Reanalysis Data

The daily combined Dark Target and Deep Blue aerosol optical depth (AOD) at 550 nm (Remer et al., 2005) with a horizontal resolution of 1° × 1°, observed by the Moderate Resolution Imaging Spectroradiometer (MODIS) aboard the Terra satellite (MOD08_D3), is used to evaluate the simulated AOD in the summer of 2008. The 3-hourly three-dimensional dust mixing ratio with a horizontal resolution of 0.5° × 0.625° latitude-longitude and with 72 vertical levels obtained from the Modern-Era Retrospective Analysis for Research and Applications, version 2 (MERRA-2) reanalysis (Randles et al., 2017) is used to evaluate the simulated dust mixing ratio in the summer of 2008.

2.2. Experimental Setup

The NICAM coupled online with the Spectral Radiation-Transport Model for Aerosol Species (SPRINTARS) (Satoh et al., 2008, 2014; Suzuki et al., 2008; Tomita & Satoh, 2004) is used to detect new transport pathways and quantify the contributions of different dust sources to the GTDL. (The detailed model description in Text S1 in Supporting Information S1.) The dust emission coefficients and critical values of soil moisture around the main global deserts are set depending on 10 regions (Figure S1 in Supporting Information S1) in the model, combined with the near-surface wind speed, the vegetation, and leaf area index, to calculate the dust emissions (Dai et al., 2018). Using the normal dust emission coefficients (Table S1 in Supporting Information S1), the control experiment was carried out to evaluate the accuracy of the NICAM (Text S2 and Figures S2 and S3 in Supporting Information S1). According to the spatial distribution of dust AOD in the control experiment (Figure S2d in Supporting Information S1), we selected four main dust sources to analyze their contributions to the GTDL. By only retaining the dust emission coefficients of regions 2, 4, 6, and 7, respectively, and setting the dust emission coefficients of other regions to 0, the individual dusts originating from North Africa (NAF), Middle East (ME), Northwestern East Asia (NWEA), and Indian Peninsula (IND) are obtained correspondingly (Figure S4 in Supporting Information S1).
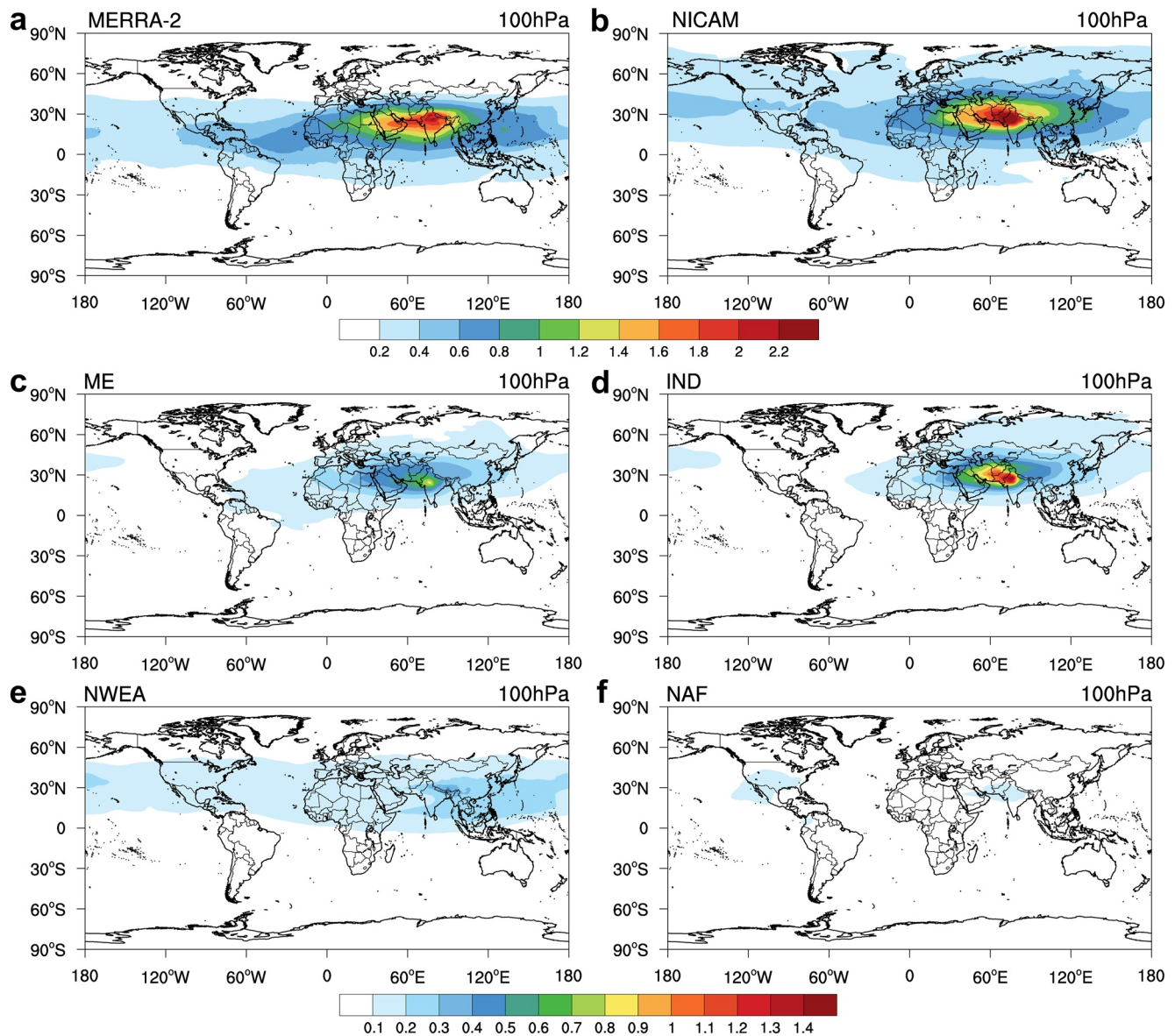
Figure 1. Spatial distributions of the dust mass concentration. Spatial distributions of the average dust mass concentration (μg kg^{-1}) at 100 hPa (a) derived from Modern-Era Retrospective Analysis for Research and Applications, version 2 (MERRA-2) and (b) simulated by Nonhydrostatic ICosahedral Atmospheric Model (NICAM) during the summer of 2008. (c) The average mass concentration of dusts originating from Middle East (ME) at 100 hPa simulated by NICAM during the summer of 2008. (d), (e), and (f) Same as (c), but for mass concentrations of dusts originating from Indian Peninsula (IND), Northwestern East Asia (NWEA), and North Africa (NAF), respectively.

3. Results

3.1. Distributions and Attributions of the GTDL

As shown in Figures 1a and 1b, the existence of an extensive GTDL which is centered on North Africa to East Asia and expands globally can be found in both reanalysis data and the simulation, and as indicated by the spatial distributions of averaged dust mass concentration during the summer of 2008, dusts originating from different sources are found at 100 hPa (Figures 1c–1f). High mass concentrations of dusts originating from ME and IND at 100 hPa are found spanning NAF, ME, IND, and East Asia, with the high-value centers appear the southwestern slope of the TP (Figures 1c and 1d). The dusts originating from NWEA show a complete encirclement of the globe with relatively low mass concentrations (Figure 1e). For the dusts from NAF, the mass concentrations at 100 hPa are the smallest among the four dust sources. However, as shown

in Figure 1f, two dust mass concentration centers can be found over the southern slope of the TP and the Rocky Mountains, which are different from dusts from other sources.

The spatial distributions of dust mass concentrations at 150 hPa are different from those at 100 hPa. In addition to a high-value center similar to 100 hPa, the dusts originating from ME at 150 hPa also with a high-value center located over Central Africa (Figure S5a in Supporting Information S1). For dusts originating from IND, the spatial distribution of mass concentrations at 150 hPa is almost identical to that at 100 hPa (Figure S5b in Supporting Information S1). Dusts originating from NWEA are transported eastward with the center of the north TP, and these dusts cross the Pacific Ocean to North America and even cover the globe at 150 hPa (Figure S5c in Supporting Information S1). Similar to the spatial distributions of dust mass concentrations at 100 hPa, dusts originating from NAF at 150 hPa are also divided into two regions, one from North Africa to East Asia and the other coves Central Africa to the Americas, with the Rocky Mountains and Central Africa as the centers (Figure S5d in Supporting Information S1).

3.2. Formation and Transport Pathways of the GTDL

The distributions of dust mass concentration at tropopause closely attribute to the atmospheric circulations, the distributions of dust mass concentration at lower layers and the vertical velocities. As indicated in Figure 61 in Supporting Information S1, under the influence of the Indian monsoon and the equatorial easterly winds, dusts originating from ME are transported eastward to the southern slope of the TP and westward to Africa at 600 hPa, respectively. The transport of dusts originating from IND is similar to that of dusts originating from ME. However, compared with ME, the location of IND is easterly and dust mass concentrations are lower, the transport of dusts from IND to Africa is weaker than that from ME (Figure S6b on Supporting Information S1). Dusts originating from NWEA are mainly transported eastward by the westerly wind belt, small amounts of dusts can be transported to the eastern slope of the TP with the northwesterly winds (Figure S6c in Supporting Information S1). The spatial distributions of horizontal circulations and dusts originating from NAF at 600 hPa are presented in Figure S6d in Supporting Information S1, indicating most of the dusts are transported across the Atlantic to the Americas by the equatorial easterly winds, and small amounts of dusts are transported to Europe and Asia by the westerly belt and the Indian monsoon, some of them can reach the southern slope of the TP (Figure S6d in Supporting Information S1).

The distributions of dust mass concentration in the lower layer indicate that dusts originating from these four dust sources can be transported to the regions around the TP with different mass concentrations. According to the longitude-height sections along 30°N (Figures 2a–2d), significant high dust mass concentration regions through the surface to the tropopause are detected over the southwestern slope of the TP, implying the southwestern slope of the TP is an important transport pathway for dusts transported from sources to the tropopause (the purple rectangles in Figure 2). The dust source of IND is closest to the southwestern slope of the TP and the dusts originating from IND can be transported to the southwestern slope of the TP with the most substantial concentrations (Figure S6b in Supporting Information S1 and Figure 2b), therefore, the corresponding transport of dusts from surface to the tropopause through this transport pathway is the largest and the vertical layer that dusts can reach is the highest (Figure 2b). The dusts originating from ME are similar to those from IND; however, the distance between ME and the TP is farther than that between IND and the TP, the mass concentration of dusts reaching the southwestern slope of the TP is lower and the dusts transported from ME to the tropopause through the southwestern slope of the TP is weaker (Figure 2a) than those from IND. The transport of the dusts from ME and IND through the southwestern slope of the TP to the tropopause corresponds to the high mass concentration centers over the southwestern slope of the TP in the spatial distribution of the GTDL at 100 hPa (Figures 1c and 1d).

Due to the obstruction of the TP, small amounts of dusts originating from NWEA can be transported to the eastern and southwestern slopes of the TP, and the contribution of dusts originating from NWEA to the GTDL through the eastern and southwestern slopes of the TP is relatively small (Figure 2c). Unlike dusts originating from other sources, as shown in Figure 2d, dusts originating from NAF are transported to the tropopause through two pathways: one is the southwestern slope of the TP and the other is the Rocky Mountains (the black rectangles in Figure 2d), which is attributable to dusts transport to these two regions at lower layers (Figure S6d in Supporting Information S1) and updrafts in these two regions (Figure S7 in Supporting Information S1 and Figure 2d). The transport of dusts from NAF through the southwestern
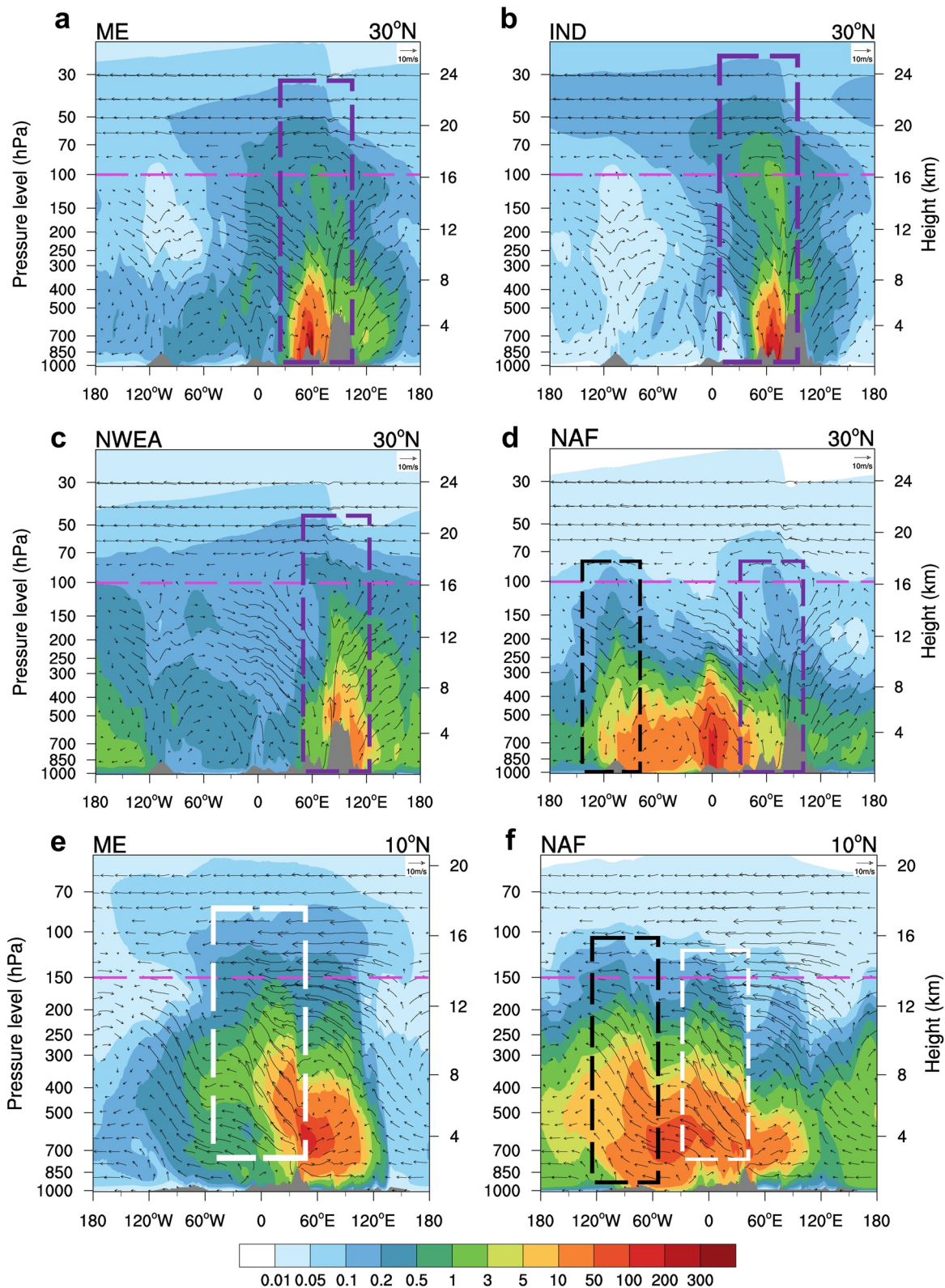
Figure 2.

slope of the TP and the Rocky Mountains to the tropopause correspond to the mass concentration centers over these two regions in the spatial distribution of the GTDL at 100 hPa (Figure 1f), which indicates the Rocky Mountains are also a transport pathway of the GTDL. However, due to the mass concentration of dusts transported to the southwestern slope of the TP is small (Figure S6d in Supporting Information S1) and the relatively weak updrafts over the Rocky Mountains (Figure S7 in Supporting Information S1), dusts transported from NAF to the tropopause is minimal.

Dusts originating from ME transported westward can also be lifted to the tropopause through other transport pathway. The longitude-height section along 10°N (Figure 2e) demonstrates that the dusts transported westward from ME to Africa can be lifted to the tropopause by strong updrafts caused by the topography of the Ethiopian Plateau (located at 5°–18°N, 30°–50°E, the white rectangles in Figure 2e). As dusts originating from ME are transported westward and upward with relatively high concentrations, a high dust mass concentration center over Central Africa at 150 hPa is formed (Figure S5a in Supporting Information S1 and Figure 2e). Dusts originating from IND can also be transported to Africa; however, the mass concentration of these dusts is small, so the dusts originating from IND cannot form a high dust concentration center over Central Africa at 150 hPa (Figure S5b in Supporting Information S1). Due to the transport of dusts originating from NAF at lower layer and updrafts over the Ethiopian Plateau and Rocky Mountains, two high mass concentration value regions are formed over Central Africa and the Rocky Mountains at 150 hPa (Figure S5d in Supporting Information S1 and Figure 2f). According to the sections of the dust mass concentration along 10°N (Figures 2e and 2f) and the spatial distributions of the dust mass concentration at 150 hPa (Figure S5 in Supporting Information S1), the Ethiopian Plateau is also a transport pathway of the GTDL.

The latitude-height sections along 82.5°E also show that southwestern slope of the TP is a key transport pathway (Figure S8 in Supporting Information S1). Furthermore, large amounts of dusts accumulate over the northern slope of the TP, but due to the downdrafts over the Taklamakan Desert and the relatively weak updrafts over the northern slope of the TP (Figures S7 and S8c in Supporting Information S1), mass concentration of dusts transported through the northern slope of the TP to the tropopause is lower than that transported through the southwestern slope of the TP to the tropopause (Figure S8c in Supporting Information S1).

3.3. Contributions of Different Dust Sources to the GTDL

The mass concentration percentages of dusts originating from the four dust sources in different layers are presented in Figure 3. Above 150 hPa, the percentage of dusts originating from IND is the largest (the red line), followed by those of dusts originating from ME (the orange line) and NWEA (the blue line), and the percentage of dusts originating from NAF is the smallest (the black line). The percentages of dust mass concentration from different sources in different layers are significantly distinct: the percentage of dusts originating from NAF is the largest (40.8%) at 800 hPa, however, the percentage plummets to 0.0% at 75 hPa (Figure 3 and Table S2 in Supporting Information S1). In contrast, the percentage of dusts originating from IND is 16.9% at 800 hPa, and the percentage surges to the largest (40.3%) at 75 hPa (Figure 3 and Table S2 in Supporting Information S1). This large variation is the result of the different distances between the different dust sources and the transport pathways. Although the mass concentration of dusts originating from NAF is largest at lower layers, the TP and the Rocky Mountains are both far from NAF, so only small amounts of dust aerosols can reach these two transport pathways after being transported over long distances, causing the percentage to decrease dramatically in the GTDL. However, other aerosol sources are closer to the transport pathways, even though the mass concentrations of dusts originating from these sources are relatively

Figure 2. Longitude-height cross sections of the dust mass concentration and vertical circulations. (a) The average mass concentration (shading; $\mu g \ kg^{-1}$) of dusts originating from Middle East (ME) and vertical circulations (vectors; m s^{-1}) along 30°N simulated by Nonhydrostatic ICosahedral Atmospheric Model (NICAM) during the summer of 2008. (b), (c), and (d) Same as (a), but for mass concentrations of dusts originating from Indian Peninsula (IND), Northwestern East Asia (NWEA), and North Africa (NAF), respectively. (e) Same as (a) but for section along 10°N. (f) Same as (e), but for mass concentrations of dusts originating from NAF. The vertical velocity is multiplied by 1,000 to make it comparable to the horizontal wind. The rectangles indicate the locations of the transport pathways. The southwestern slope of the Tibetan Plateau (TP), the Rocky Mountains, and the Ethiopian Plateau are represented by the purple rectangles, the black rectangles, and the white rectangles, respectively. The purple lines in (a)–(d) denote the 100 hPa layer, and the purple lines in (e)–(f) denote the 150 hPa layer.
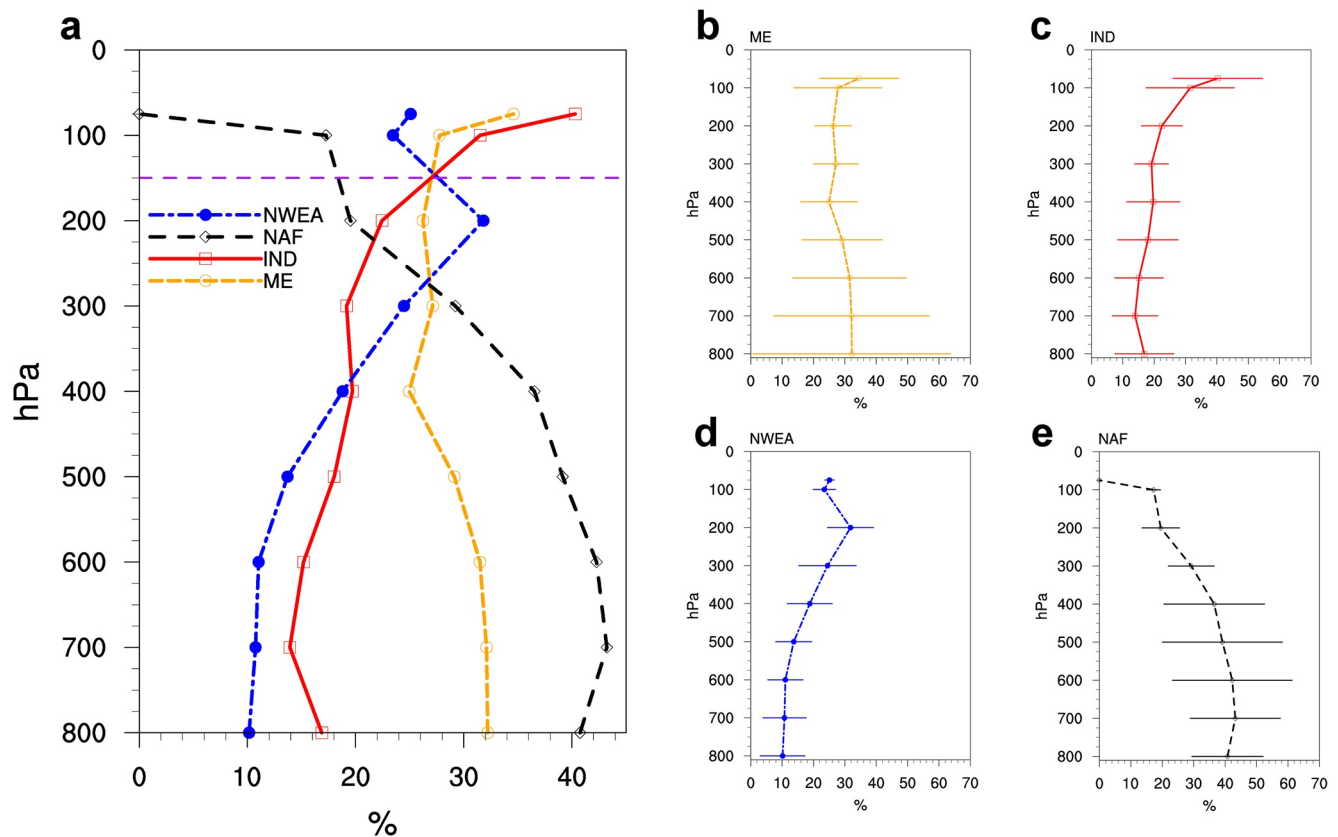
Figure 3. Profiles of the dust mass concentration percentage. (a) Mass concentration percentage (%) of dusts originating from different sources at the vertical layers. (b) Mass concentration percentage of dusts originating from Middle East (ME) at the vertical layers. (c), (d), and (e) Same as (b), but for percentage of dusts originating from Indian Peninsula (IND), Northwestern East Asia (NWEA), and North Africa (NAF), respectively. Error bars in (b)–(e) correspond to the uncertainties. The purple line denotes the 150 hPa layer.

low at lower layers, the percentages of them are still high in the GTDL, especially for dusts originating from IND.

In addition, we also quantify the contributions of different dust sources to the regional tropopause dust layers (TDLs) over the Asian, African, and American continents (Figure S9 in Supporting Information S1) where the GTDL mainly distributes. All these four dust sources can contribute to the Asian, African, and American TDLs. The contribution of dusts originating from IND to the Asian TDL is the largest (Figure S10a in Supporting Information S1). For African TDL, the contribution of dusts originating from ME is the largest at 150 hPa (Figure S10b in Supporting Information S1), which is consistent with the high-value center of dusts originating from ME over Central Africa at 150 hPa (Figure S5a in Supporting Information S1). At 100 and 75 hPa, the contributions of dusts originating from IND remain the largest. Unlike the TDLs over Asian and African continents, the contributions of dusts originating from NAF to American TDL at 150 and 100 hPa are more substantial (Figure S10c in Supporting Information S1), and the contribution of dusts originating from NWEA to American TDL is the largest (Figure S10c in Supporting Information S1).

4. Conclusions

Some studies have analyzed regional TAL using satellite observations, in-situ measurements, and reanalysis data (Lau et al., 2018; Vernier et al., 2011; Yu et al., 2017). This study takes a completely different approach by separating the dust sources in the model and simulating each one separately, and obtains some novel and interesting results. By simulating dust aerosols of each dust source separately, two new transport pathways besides the TP are detected and the contributions of different dust sources to the GTDL are quantified. Figure 4 summarizes the conclusions in this study. The TP is indeed a powerful transport pathway, especially
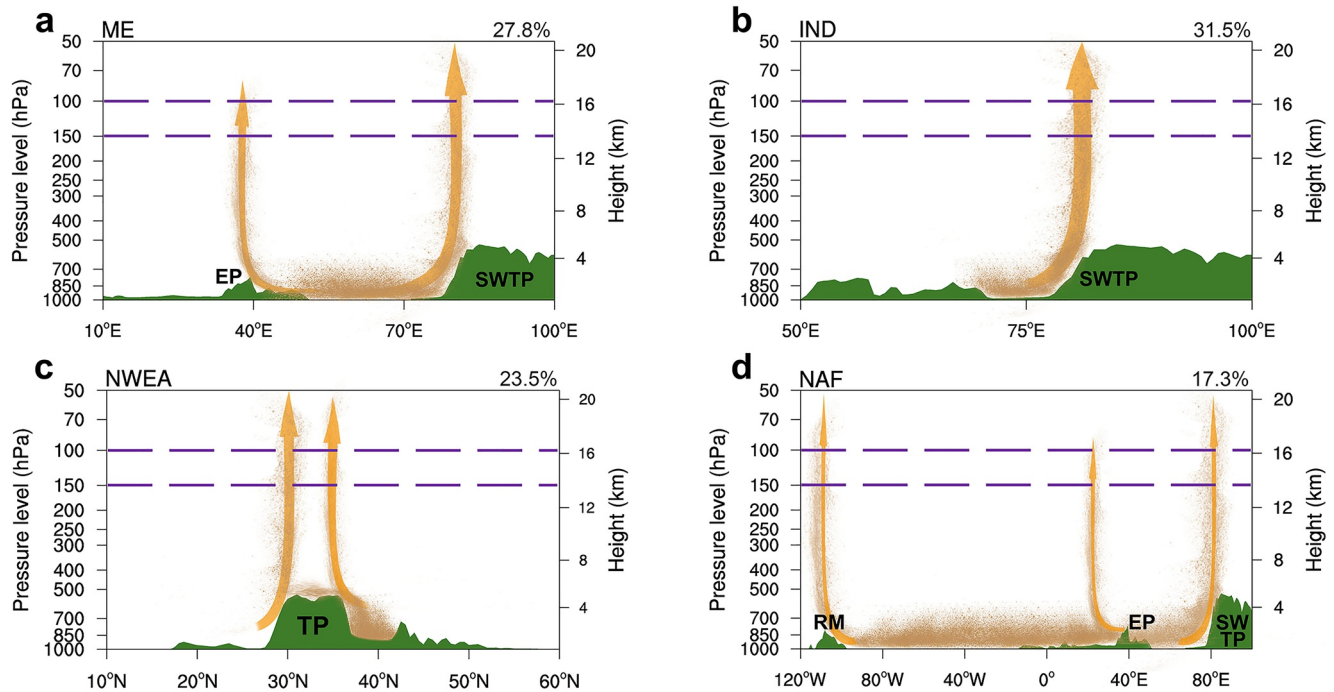
Figure 4. Schematic illustration of the dust transport to the global tropopause dust layer (GTDL). Transport of dusts originating from (a) Middle East (ME), (b) Indian Peninsula (IND), (c) Northwestern East Asia (NWEA), and (d) North Africa (NAF) to the GTDL. The yellow arrows represent the transport pathways, the numbers in the upper left corner represent the contributions of the dust sources to the GTDL at 100 hPa. EP represents the Ethiopian Plateau, SWTP represents the southwestern slope of the Tibetan Plateau (TP) and RM represents the Rocky Mountains. The green shadings mean the topographic altitude. The purple lines denote the 100 and 150 hPa layers.

its southwestern slope. In addition, the Ethiopian Plateau and Rocky Mountains also serve as transport pathways. Dusts originating from IND can be transported to the GTDL through the southwestern slope of the TP, and the contribution of them to the GTDL at 100 hPa is the largest (Figure 4b). The dust originating from ME is the second largest contributor to the GTDL at 100 hPa, and its transport pathways include the Ethiopian Plateau and the southwestern slope of the TP (Figure 4a). Dusts originating from NWEA transported to the GTDL mainly through the southwestern slope of the TP, and the northern and eastern slopes of the TP are relatively weak transport pathways (Figure 4c). The contribution of dusts originating from NAF to GTDL at 100 hPa is the smallest; however, the transport pathways of NAF are the most, including the southwestern slope of the TP, the Ethiopian Plateau, and the Rocky Mountains (Figure 4d).

Distributions of dust mass concentrations at lower layers and topography-induced updrafts are the keys to the transport of dusts to the tropopause. Large amounts of dusts at lower layers can be transported to the southwestern slope of the TP, where the updrafts are the strongest, causing the southwestern slope of the TP to become the strongest transport pathway. The northern slope of the TP also accumulates dust aerosols, but it is a weak transport pathway due to its relatively weak updrafts. Similarly, the Ethiopian Plateau is also a weak transport pathway. For the Rocky Mountains, only dusts originating from NAF with low mass concentrations can be transported here, combining with the weak updrafts, the Rocky Mountains is also a weak transport pathway.

The contributions of the dust sources to the GTDL are mainly related to the distances between the dust sources and the transport pathways. The dust sources in IND are closest to the southwestern slope of the TP, which results in dusts originating from IND can reach the southwestern slope of the TP with the largest mass concentrations; therefore, the contribution of IND to the GTDL is the largest, even though mass concentration of dusts originating from IND is small at lower layers. In contrast, mass concentration of dust aerosols originating from NAF is largest at lower layers, but the contribution of NAF to the GTDL is minimal, due to it is far from the transport pathways.

Since the satellite observations and reanalysis data cannot separate the contributions of different dust sources to the tropopause dust layers, their results mask weak transport pathways. Therefore, in order to better understand the GTDL, it is necessary to divide the dust sources for separate simulations. In addition, to obtain evidences of the new transport pathways, the ground observations (Che, Gui, et al., 2019; Che, Xia, et al., 2019), and airborne experiments over the transport pathways identified in this study need to be conducted. Moreover, Lau and Kim (2006) and Lau et al. (2006) reported that, because of the absorption of dusts over northern India, the atmosphere over northern India, and southern TP is heated relative to the region to the south, causing an anomalous large-scale circulation with rising motion over northern India and sinking motion over the northern Indian Ocean. This anomalous circulation can enhance the vertical transport of dust through southwestern slope of the TP, implying a positive feedback between dust particles and their transport pathways. Therefore, the feedback effects of dust particles on the new transport pathways, the Rocky Mountains, and the Ethiopian Plateau, will be also worth discussing in future studies.

Data Availability Statement

The MODIS product can be accessed at (https://ladsweb.modaps.eosdis.nasa.gov/search/order/2/MOD08_D3--61/2008-06-01..2008-08-31/DB/World). The MERRA-2 reanalysis data were obtained from NASA (https://goldsmr5.gesdisc.eosdis.nasa.gov/data/MERRA2/M2I3NVAER.5.12.4/2008/). All model simulation output used for this research can be downloaded from https://zenodo.org/record/5482253#.YTcVS_nA75k. The code of NICAM model used in this study can get from http://nicam.jp/tutorial/.

References

Bergman, J. W., Jensen, E. J., Pfister, L., & Yang, Q. (2012). Seasonal differences of vertical-transport efficiency in the tropical tropopause layer: On the interplay between tropical deep convection, largescale vertical ascent, and horizontal circulations. *Journal of Geophysical Research*, *117*, D05302. https://doi.org/10.1029/2011JD016992

Bian, J., Li, D., Bai, Z., Li, Q., Lyu, D., & Zhou, X. (2020). Transport of Asian surface pollutants to the global stratosphere from the Tibetan Plateau region during the Asian summer monsoon. *National Science Review*, *7*, 516–533. https://doi.org/10.1093/nsr/nwaa005

Bossolasco, A., Jegou, F., Sellitto, P., Berthet, G., Legras, B., & Legras, B. (2021). Global modeling studies of composition and decadal trends of the Asian tropopause aerosol layer. *Atmospheric Chemistry and Physics*, *21*(4), 2745–2764. https://doi.org/10.5194/acp-21-2745-2021

Chao, X., Ma, Y. M., Yang, K., & Chao, Y. (2018). Tibetan Plateau impacts on global dust transport in the upper troposphere. *Journal of Climate*, *31*(12), 4745–4756. https://doi.org/10.1175/JCLI-D-17-0313.1

Che, H., Gui, K., Xia, X., Wang, Y., Holben, B., Goloub, P., et al. (2019). Large contribution of meteorological factors to inter-decadal changes in regional aerosol optical depth. *Atmospheric Chemistry and Physics*, *19*, 10497–10523. https://doi.org/10.5194/acp-19-10497-2019

Che, H., Xia, X., Zhao, H., Dubovik, O., Holben, B., Goloub, P., et al. (2019). Spatial distribution of aerosol microphysical and optical properties and direct radiative effect from the china aerosol remote sensing network. *Atmospheric Chemistry and Physics*, *19*, 11843–11864. https://doi.org/10.5194/acp-19-11843-2019

Dai, T., Cheng, Y. M., Zhang, P., Shi, G. Y., Sekiguchi, M., Suzuki, K., et al. (2018). Impacts of meteorological nudging on the global dust cycle simulated by NICAM coupled with an aerosol model. *Atmospheric Environment*, *190*, 99–115. https://doi.org/10.1016/j.atmosenv.2018.07.016

Dessler, A. E., Schoeberl, M. R., Wang, T., Davis, S. M., & Rosenlof, K. H. (2013). Stratospheric water vapor feedback. *Proceedings of the National Academy of Sciences of the United States of America*, *110*(45), 18087–18091. https://doi.org/10.1073/pnas.1310344110

Fadnavis, S., Schultz, M. G., Semeniuk, K., Mahajan, A. S., Pozzoli, L., Sonbawne, S., et al. (2014). Trends in peroxyacetyl nitrate (PAN) in the upper troposphere and lower stratosphere over southern Asia during the summer monsoon season: Regional impacts. *Atmospheric Chemistry and Physics*, *14*, 12725–12743. https://doi.org/10.5194/acp-14-12725-2014

Fadnavis, S., Semeniuk, K., Pozzoli, L., Schultz, M. G., Ghude, S. D., Das, S., & Kakatkar, R. (2013). Transport of aerosols into the UTLS and their impact on the Asian monsoon region as seen in a global model simulation. *Atmospheric Chemistry and Physics*, *13*, 8771–8786. https://doi.org/10.5194/acp-13-8771-2013

Fairlie, T. D., Liu, H., Vernier, J.-P., Campuzano-Jost, P., Jimenez, J. L., Jo, D. S., et al. (2020). Estimates of regional source contributions to the Asian tropopause aerosol layer using a chemical transport model. *Journal of Geophysical Research: Atmospheres*, *125*, e2019JD031506. https://doi.org/10.1029/2019JD031506

Frey, W., Schofield, R., Hoor, P., Kunkel, D., Ravegnani, F., Ulanovsky, A., et al. (2015). The impact of overshooting deep convection on local transport and mixing in the tropical upper troposphere/lower stratosphere (UTLS). *Atmospheric Chemistry and Physics*, *15*, 6467–6486. https://doi.org/10.5194/acp-15-6467-2015

Fu, R., Hu, Y., Wright, J. S., Jiang, J. H., Dickinson, R. E., Chen, M., et al. (2006). Short circuit of water vapor and polluted air to the global stratosphere by convective transport over the Tibetan Plateau. *Proceedings of the National Academy of Sciences of the United States of America*, *103*, 5664–5669. https://doi.org/10.1073/pnas.0601584103

Gu, Y., Liao, H., & Bian, J. (2016). Summertime nitrate aerosol in the upper troposphere and lower stratosphere over the Tibetan Plateau and the South Asian summer monsoon region. *Atmospheric Chemistry and Physics*, *16*, 6641–6663. https://doi.org/10.5194/acp-16-6641-2016

Hoinka, K. P. (1997). The tropopause: Discovery, definition and demarcation. *Meteorologische Zeitschrift*, *6*(6), 281–303. https://doi.org/10.1127/metz/6/1997/281

Holton, J. R., Haynes, P. H., McIntyre, M. E., Douglass, A. R., Rood, R. B., & Pfister, L. (1995). Stratosphere-troposphere exchange. *Reviews of Geophysics*, *33*, 403–440. https://doi.org/10.1029/95RG02097

Kar, J., Bremer, H., Drummond, J. R., Rochon, Y. J., Jones, D., Nichitiu, F., et al. (2004). Evidence of vertical transport of carbon monoxide from Measurements of Pollution in the Troposphere (MOPITT). *Geophysical Research Letters*, *31*, L23105. https://doi.org/10.1029/2004GL021128

Lau, K. M., & Kim, K. M. (2006). Observational relationships between aerosol and Asian monsoon rainfall, and circulation. *Geophysical Research Letters*, *33*, 320–337. https://doi.org/10.1029/2006GL027546

Lau, K. M., Kim, M. K., & Kim, K. M. (2006). Asian summer monsoon anomalies induced by aerosol direct forcing: The role of the Tibetan Plateau. *Climate Dynamics*, *26*, 855–864. https://doi.org/10.1007/s00382-006-0114-z

Lau, W. K. M., Yuan, C., & Li, Z. (2018). Origin, maintenance and variability of the Asian Tropopause Aerosol Layer (ATAL): The roles of monsoon dynamics. *Scientific Reports*, *8*, 3960–3973. https://doi.org/10.1038/s41598-018-22267-z

Legras, B., & Bucci, S. (2020). Confinement of air in the Asian monsoon anticyclone and pathways of convective air to the stratosphere during the summer season. *Atmospheric Chemistry and Physics*, *20*, 11045–11064. https://doi.org/10.5194/acp-20-11045-2020

Li, Q. B., Jiang, J. H., Wu, D. L., Read, W. G., Livesey, N. J., Waters, J. W., et al. (2005). Convective outflow of South Asian pollution: A global CTM simulation compared with EOS MLS observations. *Geophysical Research Letters*, *32*, L14826. https://doi.org/10.1029/2005GL022762

Ma, J., Brühl, C., He, Q., Steil, B., Karydis, V. A., Klingmüller, K., et al. (2019). Modeling the aerosol chemical composition of the tropopause over the Tibetan Plateau during the Asian summer monsoon. *Atmospheric Chemistry and Physics*, *19*, 11587–11612. https://doi.org/10.5194/acp-19-11587-2019

Neely, R. R., Yu, P., Rosenlof, K. H., Toon, O. B., Daniel, J. S., Solomon, S., & Miller, H. L. (2014). The contribution of anthropogenic SO_2 emissions to the Asian tropopause aerosol layer. *Journal of Geophysical Research: Atmospheres*, *119*, 1571–1579. https://doi.org/10.1002/2013JD020578

Pan, L. L., Honomichl, S. B., Kinnison, D. E., Abalos, M., Randel, W. J., Bergman, J. W., & Bian, J. (2016). Transport of chemical tracers from the boundary layer to stratosphere associated with the dynamics of the Asian summer monsoon. *Journal of Geophysical Research: Atmospheres*, *121*, 14159–14174. https://doi.org/10.1002/2016JD025616

Park, M., Randel, W. J., Emmons, L. K., & Livesey, N. J. (2009). Transport pathways of carbon monoxide in the Asian summer monsoon diagnosed from Model of Ozone and Related Tracers (MOZART). *Journal of Geophysical Research*, *114*, D08303. https://doi.org/10.1029/2008JD010621

Park, M., Randel, W. J., Kinnison, D. E., Garcia, R. R., & Choi, W. (2004). Seasonal variation of methane, water vapor, and nitrogen oxides near the tropopause: Satellite observations and model simulations. *Journal of Geophysical Research*, *109*, D03302. https://doi.org/10.1029/2003JD003706

Randel, W. J., & Jensen, E. J. (2013). Physical processes in the tropical tropopause layer and their roles in a changing climate. *Nature Geoscience*, *6*, 169–176. https://doi.org/10.1038/ngeo1733

Randel, W. J., Park, M., Emmons, L., Kinnison, D., Bernath, P., Walker, K. A., et al. (2010). Asian monsoon transport of pollution to the stratosphere. *Science*, *328*, 611–613. https://doi.org/10.1126/science.1182274

Randles, C. A., Sliva, A., Buchard, V., Colarco, P. R., Flynn, C. J., Govindaraju, R., et al. (2017). The MERRA-2 aerosol reanalysis, 1980-onward, Part I: System description and data assimilation evaluation. *Journal of Climate*, *30*(17), 6823–6850. https://doi.org/10.1175/JCLI-D-16-0609.1

Remer, L. A., Kaufman, Y. J., Tanré, D., Mattoo, S., Chu, D. A., Martins, J. V., et al. (2005). The MODIS aerosol algorithm, products, and validation. *Journal of the Atmospheric Sciences*, *62*, 947–973. https://doi.org/10.1175/JAS3385.1

Satoh, M., Matsuno, T., Tomita, H., Miura, H., Nasuno, T., & Iga, S. (2008). Nonhydrostatic icosahedral atmospheric model (NICAM) for global cloud resolving simulations. *Journal of Computational Physics*, *227*, 3486–3514. https://doi.org/10.1016/j.jcp.2007.02.006

Satoh, M., Tomita, H., Yashiro, H., Miura, H., Kodama, C., Seiki, T., et al. (2014). The non-hydrostatic icosahedral atmospheric model: Description and development. *Progress in Earth and Planetary Science*, *1*(1), 18. https://doi.org/10.1186/s40645-014-0018-1

Suzuki, K., Nakajima, T., Satoh, M., Tomita, H., Takemura, T., Nakajima, T. Y., & Stephens, G. L. (2008). Global cloud-system-resolving simulation of aerosol effect on warm clouds. *Geophysical Research Letters*, *35*, 35610–35616. https://doi.org/10.1029/2008GL035449

Tissier, A. S., & Legras, B. (2016). Convective sources of trajectories traversing the tropical tropopause layer. *Atmospheric Chemistry and Physics*, *16*, 3383–3398. https://doi.org/10.5194/acp-16-3383-2016

Tomita, H., & Satoh, M. (2004). A new dynamical framework of nohydrostatic global model using the icosahedral grid. *Fluid Dynamics Research*, *34*(6), 357–400. https://doi.org/10.1016/j.fluiddyn.2004.03.003

Uno, I., Eguchi, K., Yumimoto, K., Takemura, T., Shimizu, A., Uematsu, M., et al. (2009). Asian dust transported one full circuit around the globe. *Nature Geoscience*, *2*, 557–560. https://doi.org/10.1038/ngeo583

Vernier, J. P., Fairlie, T. D., Natarajan, M., Wienhold, F. G., Bian, J., Martinsson, B. G., et al. (2015). Increase in upper tropospheric and lower stratospheric aerosol levels and its potential connection with Asian pollution. *Journal of Geophysical Research: Atmospheres*, *120*, 1608–1619. https://doi.org/10.1002/2014JD022372

Vernier, J. P., Thomason, L. W., & Kar, J. (2011). CALIPSO detection of an Asian tropopause aerosol layer. *Geophysical Research Letters*, *38*, L07804. https://doi.org/10.1029/2010GL046614

Vogel, B., Günther, G., Müller, R., Grooß, J.-U., & Riese, M. (2015). Impact of different Asian source regions on the composition of the Asian monsoon anticyclone and of the extratropical lowermost stratosphere. *Atmospheric Chemistry and Physics*, *15*, 13699–13716. https://doi.org/10.5194/acp-15-13699-2015

Winker, D. M., Vaughan, M. A., Omar, A., Hu, Y., Powell, K. A., Liu, Z., et al. (2009). Overview of the CALIPSO mission and CALIOP data processing algorithms. *Journal of Atmospheric and Oceanic Technology*, *26*(11), 2310–2323. https://doi.org/10.1175/2009JTECHA1281.1

Wen, H., Zhou, Y., Xu, X., Wang, T., Chen, Q., et al. (2021). Water-soluble brown carbon in atmospheric aerosols along the transport pathway of Asian dust: Optical properties, chemical compositions, and potential sources. *Science of The Total Environment*, *789*, 147971. https://doi.org/10.1016/j.scitotenv.2021.147971

Xu, C., Ma, Y. M., You, C., & Zhu, Z. K. (2015). The regional distribution characteristics of aerosol optical depth over the Tibetan Plateau. *Atmospheric Chemistry and Physics*, *15*, 12065–12078. https://doi.org/10.5194/acp-15-12065-2015

Yu, P., Rosenlof, K. H., Shang, L., Telg, H., Gao, R. S., Rollins, A. W., et al. (2017). Efficient transport of tropospheric aerosol into the stratosphere via the Asian summer monsoon anticyclone. *Proceedings of the National Academy of Sciences of the United States of America*, *114*(27), 6972–6977. https://doi.org/10.1073/pnas.1701170114

Yu, P., Toon, O. B., Neely, R. R., Martinsson, B. G., & Brenninkmeijer, C. A. M. (2015). Composition and physical properties of the Asian Tropopause Aerosol Layer and the North American Tropospheric Aerosol Layer. *Geophysical Research Letters*, *42*, 2540–2546. https://doi.org/10.1002/2015GL063181

Yuan, C., Lau, W. K. M., Li, Z., & Cribb, M. (2019). Relationship between Asian monsoon strength and transport of surface aerosols to the Asian Tropopause Aerosol Layer (ATAL): Interannual variability and decadal changes. *Atmospheric Chemistry and Physics*, *19*, 1901–1913. https://doi.org/10.5194/acp-19-1901-2019

References From the Supporting Information

Dai, T., Goto, D., Schutgens, N. A. J., Dong, X., Shi, G., & Nakajima, T. (2014a). Simulated aerosol key optical properties over global scale using an aerosol transport model coupled with a new type of dynamic core. *Atmospheric Environment*, *82*, 71–82. https://doi.org/10.1016/j.atmosenv.2013.10.018

Dai, T., Schutgens, N. A. J., Goto, D., Shi, G., & Nakajima, T. (2014b). Improvement of aerosol optical properties modeling over eastern Asia with MODIS AOD assimilation in a global non-hydrostatic icosahedral aerosol transport model. *Environmental Pollution*, *195*, 319–329. https://doi.org/10.1016/j.envpol.2014.06.021

Dai, T., Shi, G., & Nakajima, T. (2015). Analysis and evaluation of the global aerosol optical properties simulated by an online aerosol-coupled non-hydrostatic icosahedral atmospheric model. *Advances in Atmospheric Sciences*, *32*(6), 743–758. https://doi.org/10.1007/s00376-014-4098-z

Lamarque, J. F., Bond, T. C., Eyring, V., Granier, C., Heil, A., Klimont, Z., et al. (2010). Historical (1850–2000) gridded anthropogenic and biomass burning emissions of reactive gases and aerosols: Methodology and application. *Atmospheric Chemistry and Physics*, *10*, 7017–7039. https://doi.org/10.5194/acp-10-7017-2010

Miyamoto, Y., Kajikawa, Y., Yoshida, R., Yamaura, T., Yashiro, H., & Tomita, H. (2013). Deep moist atmospheric convection in a sub kilometer global simulation. *Geophysical Research Letters*, *40*, 4922–4926. https://doi.org/10.1002/grl.50944

Takemura, T., Egashira, M., Matsuzawa, K., Ichijo, H., O'ishi, R., & Abe-Ouchi, A. (2009). A simulation of the global distribution and radiative forcing of soil dust aerosols at the last glacial maximum. *Atmospheric Chemistry and Physics*, *9*, 3061–3073. https://doi.org/10.5194/acp-9-3061-2009

Takemura, T., Okamoto, H., Maruyama, Y., Numaguti, A., Higurashi, A., & Nakajima, T. (2000). Global three-dimensional simulation of aerosol optical thickness distribution of various origins. *Journal of Geophysical Research*, *105*, 17853–17873. https://doi.org/10.1029/2000JD900265